

Control of Relative Tunneling Rates in Single Molecule Bipolar Electron Transport

S. W. Wu, G. V. Nazin, X. Chen, X. H. Qiu, and W. Ho*

Department of Physics and Astronomy and Department of Chemistry, University of California, Irvine, California 92697-4575, USA
(Received 25 July 2004; published 1 December 2004)

The influence of relative electron tunneling rates on electron transport in a double-barrier single-molecule junction is studied. The junction is defined by positioning a scanning tunneling microscope tip above a copper phthalocyanine molecule adsorbed on a thin oxide film grown on the NiAl(110) surface. By tuning the tip-molecule separation, the ratio of tunneling rates through the two barriers, vacuum and oxide, is controlled. This results in dramatic changes in the relative intensities of individual conduction channels, associated with different vibronic states of the molecule.

DOI: 10.1103/PhysRevLett.93.236802

PACS numbers: 73.63.-b, 63.22.+m, 68.37.Ef, 73.40.Gk

Electron transport in single-molecule junctions has recently been the focus of many research efforts, in view of its importance for molecular electronics [1–8]. Among the most important characteristics of a molecular junction are electron tunneling rates between the metal electrodes that contact the molecule and the molecule itself. The effect of relative tunneling rates on electron transport has been addressed in experiments involving quantum dot junctions [9,10] and quantum well heterostructures [11]. The appearance of features corresponding to multiple Coulomb charging in the differential conductance (dI/dV) spectra has been shown to depend on the relative tunneling rates in the junction [10]. However, the effect of relative tunneling rates on electron transport in a single-molecule junction, especially in the presence of electron-vibration coupling [2,3,12], has not been studied experimentally.

In this Letter, we use a scanning tunneling microscope (STM) to define a double-barrier junction (schematically shown in Fig. 1(a)) by positioning the STM tip over an individual copper phthalocyanine [CuPc, Fig. 1(b)] molecule adsorbed on a thin (approximately 0.5 nm [13]) insulating Al_2O_3 film grown on the NiAl(110) surface. The two tunnel barriers in the junction are the vacuum gap between the STM tip and the molecule, and the oxide film between the molecule and NiAl. Unlike the typical single-barrier (vacuum) junction for STM experiments, the finite voltage drops in both barriers lead to conduction through the same vibronic states of the molecule at opposite bias polarities—bipolar conduction [14]. However, the dI/dV spectra taken at opposite bias polarities show a distinct asymmetry. By varying the tip-molecule separation, we control the ratio of electron tunneling rates through the two tunnel barriers. This results in dramatic changes in the relative intensities of molecular vibronic states observed in the dI/dV spectra [15] and facilitates the understanding of the conductance asymmetry suggesting a two-step tunneling mechanism, where electrons first tunnel into a localized state in the junction from one electrode, and then tunnel out to the other electrode.

The experiments were conducted with a homebuilt ultrahigh-vacuum STM operated at 15 K [16]. The Al_2O_3 film was prepared by partial oxidation of the clean NiAl(110) surface. CuPc was thermally sublimed onto the oxidized surface at 15 K [12]. The surface of the Al_2O_3 film is relatively inhomogeneous [13], so that a number of different CuPc adsorption configurations are possible. Among all possible types of adsorption, here we present three types: M1, M2, and M3 [Fig. 1(c)]. These produce distinctly different STM images as well as dI/dV spectra [Fig. 1(d)]. We distinguish two different types of spectral features. Type I features are relatively broad bands seen for M1 and M2 when $V_b > 0$, and for M3 when $V_b < 0$, where V_b is the sample bias voltage with respect to the tip. These bands are attributed to tunneling through the vibronic levels of transiently charged states of CuPc, as was shown in Ref. [12] and discussed further below. Type II features are sharp peaks seen for M1 and M2 when $V_b < 0$, and for M3 when $V_b > 0$. The conductance is nearly zero between the onsets for type I and type II.

By examining the dI/dV spectra from 70 different CuPc molecules adsorbed on the oxide surface, we found that type I and type II dI/dV features are correlated, as shown in Fig. 1(e). The ratios of conductance onsets for type I and type II features were in the range of 7.1 ± 2.6 . For a fraction of the molecules, individual vibronic peaks were resolved in the type I dI/dV bands. For these molecules we plot type I onset peak versus type II sharp peak [pluses in Fig. 1(e)].

The established correlation suggests that both types of spectral features at opposite bias polarities are due to tunneling through the same molecular states (bipolar conduction), as could be expected for a double-barrier tunnel junction [conduction through the affinity level of CuPc is schematically shown in Figs. 2(a) and 2(b)]. When the sample is biased with respect to the tip, the transient charged state of CuPc responsible for electron transport is shifted by the amount corresponding to the average electrostatic potential within the molecule. The current begins to flow through the molecule when the

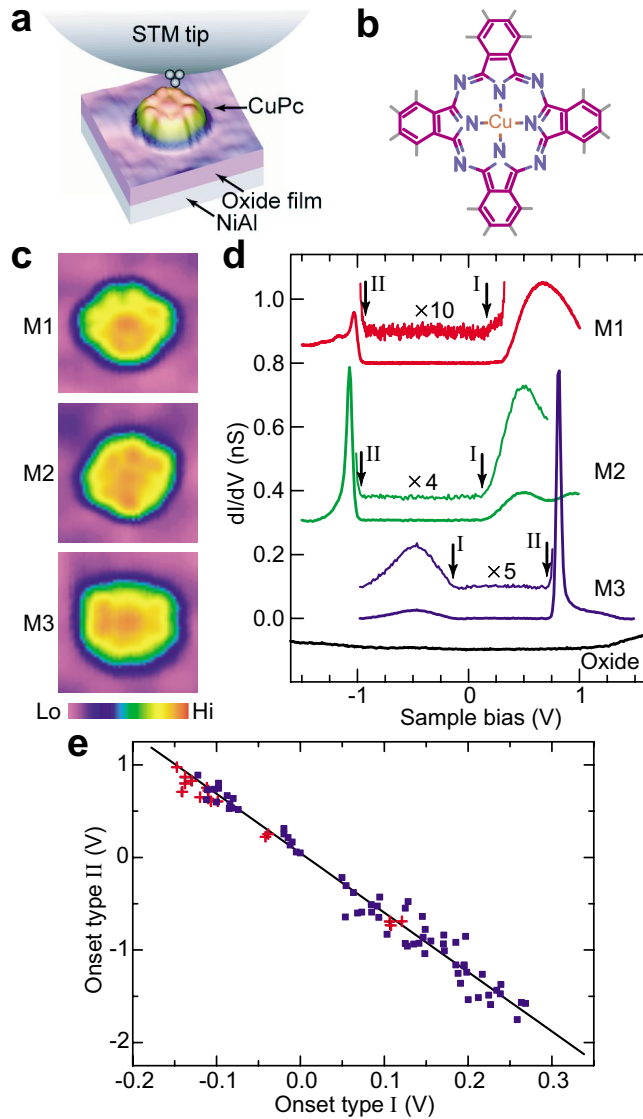


FIG. 1 (color online). (a) Schematics of a double-barrier single-molecule junction. (b) Molecular structure of CuPc. (c) STM topographic images of three different conformations of CuPc (M1, M2, and M3) adsorbed on the oxide surface. The scan size is 37 \AA by 37 \AA , $V_b = 2.0 \text{ V}$, and $I = 0.1 \text{ nA}$. (d) dI/dV spectra measured with the STM tip positioned over the center of the three molecules in (c). The conductance onsets at opposite bias polarities are marked by I (broad band onset) and II (sharp peak onset). The spectra for M1, M2, and oxide are offset for clarity. The dI/dV signal was recorded with the lock-in technique. The tunnel gap was set at $V_b = 2.0 \text{ V}$ and $I = 0.1 \text{ nA}$. The bias modulation was 10 mV (rms) at 400 Hz . (e) Plot showing the correlation of onset type I and onset type II for 70 different CuPc molecules adsorbed on oxide surface (squares) compared to the correlation of the conductance peaks (pluses).

shifted molecular energy level is aligned with the Fermi level of either the STM tip or NiAl.

The tip apex radius is much larger than the tip-NiAl distance, so that the junction has approximately parallel plate structure. From simple electrostatics (neglecting

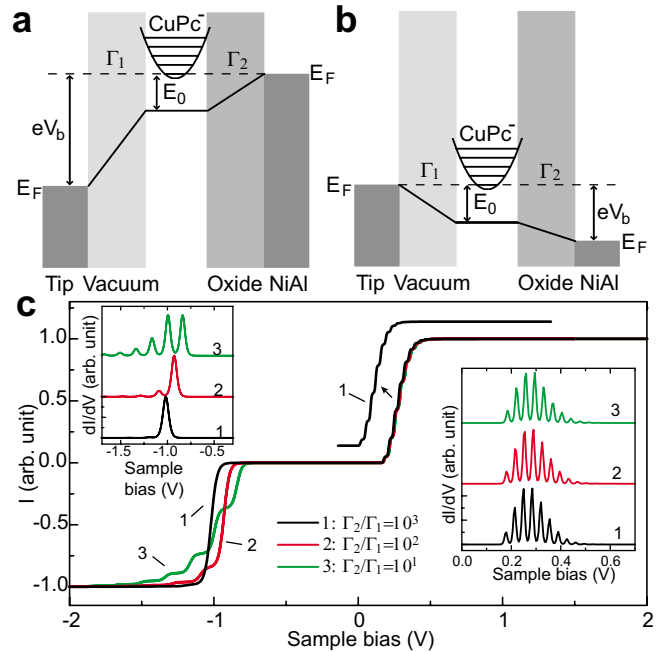


FIG. 2 (color online). (a),(b) Diagram showing the conduction through the affinity (CuPc^-) level of a CuPc under negative ($V_b < 0$) and positive ($V_b > 0$) sample bias, respectively. The electrostatic potential profiles in the junction under the influence of sample bias are shown by the solid lines. (c) Numerical simulation of $I(V)$, normalized at 2 V , based on rate equations with the inclusion of vibronic coupling for different ratios of tunneling rates [18,19]. Γ_1 , Γ_2 are the tunneling rates through the vacuum gap and oxide film, respectively. The two insets show the dI/dV spectra, scaled and offset, for opposite bias polarities. For clarity, one of the closely spaced curves for $V_b > 0$ is shown. Parameters are $g = 3$, $\hbar\omega_0 = 30 \text{ meV}$, $kT = 0.1\hbar\omega_0$, $E_0 = 0.15 \text{ V}$, and onset ratios are 5.8, 5.2, and 4.6 for curves 1, 2, and 3, respectively, where g is the Franck-Condon parameter and $\hbar\omega_0$ is the vibrational energy. Curves of similar shapes were obtained for different vibrational energies.

effect of CuPc on the resulting potential), tunneling will occur at bias voltages given by $eV_b = E_0[1 + d/(\epsilon z)]$ when the first tunneling step is between the tip and CuPc [Fig. 2(b)] and $eV_b = -E_0(1 + \epsilon z/d)$ for tunneling between NiAl and CuPc [Fig. 2(a)], where E_0 is the energy level of the molecular state with respect to the Fermi level of the unbiased junction, z is the tip-molecule separation, d is the thickness, and ϵ is the effective dielectric constant of the oxide film. The above derivation also applies to the case of tunneling through the ionization level of CuPc. The ratio of the conduction onsets is approximately given by $\epsilon z/d$, which is expected to be large because of the large effective dielectric constant of the oxide film (~ 8 for bulk alumina) and the fact that d is comparable to z . The observed ratio of onsets in Fig. 1(e) is around 7.1 ± 2.6 , which identifies type I dI/dV features as being due to the case when the first tunneling step is between the tip and CuPc, whereas

type II dI/dV features must be associated with tunneling between NiAl and CuPc. Therefore, for M1 and M2 tunneling occurs through the affinity level of CuPc, while for M3, it is through the ionization level.

At this point, it is unclear why tunneling through the same state would produce such drastically different spectral signatures (i.e., why type I conductance shows a broad band, whereas only one sharp peak is observed for type II conductance). To understand this behavior, we measured dI/dV spectra for different z .

The conduction through molecule M1 [CuPc⁻ transient state, Figs. 2(a) and 2(b)] is shown in Fig. 3. For $V_b < 0$ [Fig. 3(a)] and large z , the conductance shows only a single sharp peak (bottom curve). For smaller z , additional equally spaced peaks appear in the dI/dV (top curves), and the spectra shift to less negative V_b . All three observed peaks shift linearly with z [Fig. 3(e)], due to the factor of $1 + \frac{\epsilon z}{d}$ for type II conductance.

For $V_b > 0$ [Fig. 3(b)], the overall shape and position of the spectra did not change noticeably with z . Because of the factor $1 + \frac{d}{\epsilon z}$ for type I conductance, the shift of type I dI/dV features with z is expected to be $(\frac{\epsilon z}{d})^2$ times smaller than that of type II and is too small to be observed in Fig. 3(b).

The spectra in Fig. 3(b) contain a sequence of equidistant features attributable to the vibronic states of CuPc⁻, as demonstrated by measuring (following Ref. [12]) the d^2I/dV^2 signal [Figs. 3(c) and 3(d)]. The dependence of the peak positions and intensities in Figs. 3(a) and 3(b) on the z offset is shown in Figs. 3(e) and 3(f). The ratio for the spacings of the vibronic states at the opposite bias polarities is 4.8 ± 0.3 (at zero z offset). This is in the range for the ratio of the onsets 6.5 ± 1.8 [the corresponding magnified curve in Fig. 1(d)]. Taking into account the voltage division in the junction, the peak spacing found in Fig. 3(d) (29 ± 2 meV) gives a value of 25 ± 2 meV for the vibrational energy, which is attributable to the CuPc macrocycle bending and in-phase motion of pyrrole groups [17].

The variation of z in the case of M3 (CuPc⁺ transient state) gives similar results, as shown in Fig. 4. Type II peak ($V_b > 0$) develops a vibronic sideband with equally spaced peaks and shifts to smaller V_b when z is reduced. Similar to M1, type I dI/dV band ($V_b < 0$) maintains its structure. The spacings of vibronic states at opposite bias polarities give a ratio of 5.7 ± 0.1 at zero z offset, as compared to the onset ratio of 6.6 ± 1.5 and the ratio of 5.8 ± 0.1 for the first peaks in Figs. 4(a) and 4(b). The vibrational energy is determined to be 54 ± 2 meV, which is in the range of the out-of-plane motion of the isoindole atoms of CuPc [17].

The asymmetry in the shapes of dI/dV curves as well as their z -dependent behavior can be understood by considering a two-step tunneling process. In such a process, the relative tunneling rates, as well as the order of the two tunneling events, play a determining role in I - V charac-

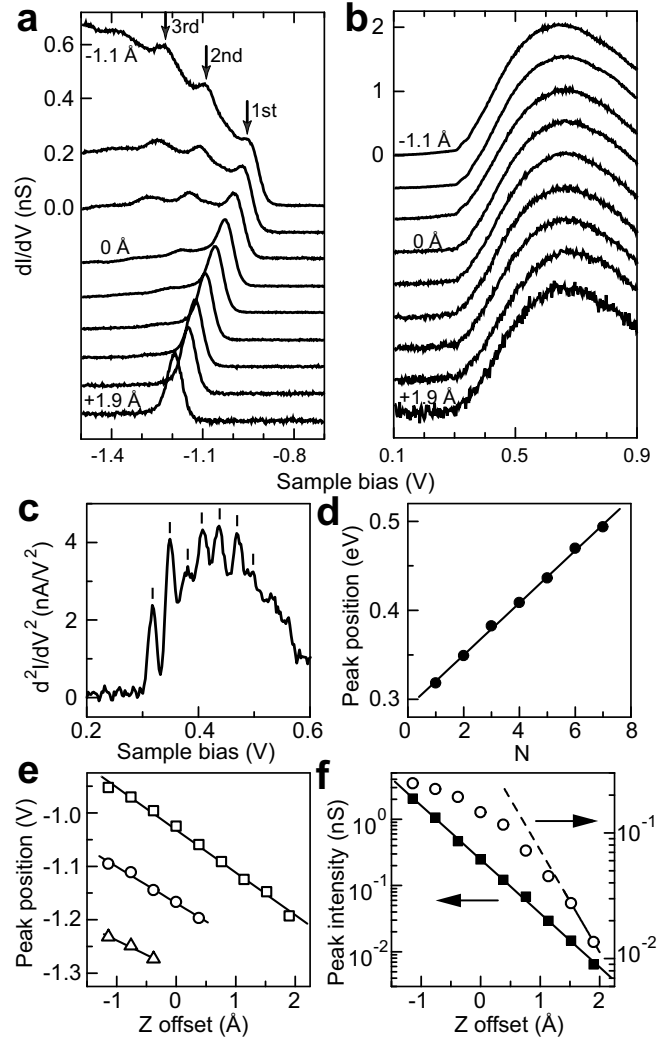


FIG. 3. (a),(b) dI/dV spectra for different tip-molecule separations (z) above molecule M1 (Fig. 1) for $V_b < 0$ and $V_b > 0$, respectively. Z offsets, referenced to the gap set with $V_b = 2.0$ V, $I = 0.1$ nA, were adjusted incrementally from -1.1 to $+1.9$ Å. The spectra (except the topmost spectra) are scaled by different factors and offset for clarity. (c) d^2I/dV^2 spectrum measured concurrently with the second spectrum from the top in (b). (d) Positions of the peaks from (c) as a function of the number of the peak. Linear fitting of the data gives the spacing of 29 ± 2 mV. (e) Peak positions observed in (a) as a function of z offset. The open squares, circles, and triangles correspond to the first, second, and third peaks marked in (a), respectively. (f) Peak intensities from (a) (open circles) and (b) (solid squares) as a function of z offset. The solid squares correspond to the band intensity maximum in (b), while the open circles correspond to the first peak intensity in (a).

teristics. This effect is simulated here with rate equations including vibronic coupling [18,19]. The results of the simulation are shown in Fig. 2(c) [20].

At large tip-molecule separation, the tunneling rate Γ_1 through the vacuum gap becomes much slower than the rate Γ_2 through the oxide film [$\Gamma_1 \ll \Gamma_2$, as in curve 1 in Fig. 2(c)]. For conduction through CuPc⁻, at $V_b > 0$

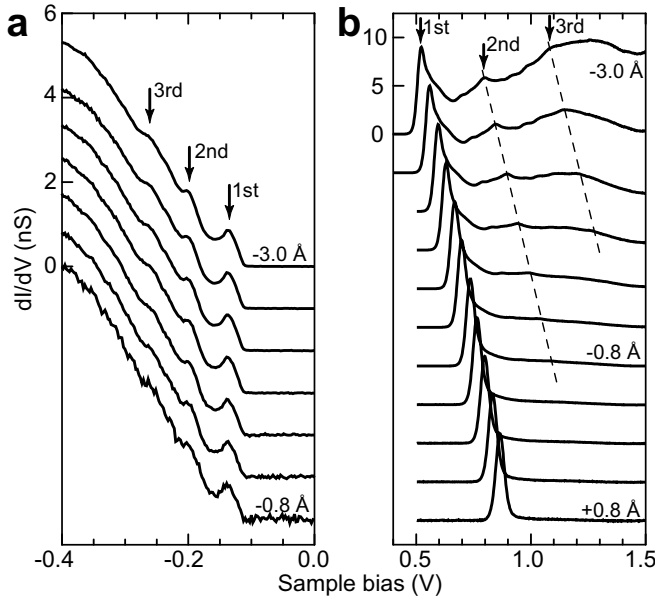


FIG. 4. (a),(b) dI/dV spectra with different tip-molecule separations over the molecule M3 (Fig. 1) for $V_b < 0$ and $V_b > 0$, respectively. The spectra (except the topmost spectra) are scaled by different factors and offset for clarity.

[Fig. 2(b)], electrons tunnel through the vacuum gap one at a time from the STM tip into the CuPc molecule, forming CuPc^- , then quickly tunnel through the oxide film to the substrate. When the bias is increased, the total current is increased as electrons begin to tunnel into the higher vibronic states with probabilities governed by the Franck-Condon principle [21]. Hence, the I - V curve exhibits a sequence of steps, and the dI/dV curve shows a progression of vibronic peaks.

In contrast, at $V_b < 0$ [Fig. 2(a)], an electron from the substrate tunnels into the molecule once the threshold V_b is reached. Higher vibronic states become available for tunneling at higher V_b and tunneling into CuPc becomes faster, but this does not lead to an increase in the current, since the current is limited by the small rate of tunneling from CuPc into the tip ($\Gamma_2 \gg \Gamma_1$). Coulomb repulsion prevents a second electron from tunneling into the molecule, so that only a single step is observed in the I - V curve, and a single sharp peak in the corresponding dI/dV curve.

As the tip-molecule separation decreases, Γ_1 increases owing to its exponential dependence on the barrier width. The sharp peak at $V_b < 0$ develops a sideband with multiple vibronic peaks [Figs. 2(c) and 3(a)] as Γ_1/Γ_2 increases. The broad band at $V_b > 0$ maintains its structure [Fig. 2(c) and 3(b)]. In the limit when $\Gamma_2 \ll \Gamma_1$, a reversal in the shapes of dI/dV characteristics would be expected: a single sharp peak at $V_b > 0$ and multiple peaks at $V_b < 0$. Because the molecule could be easily perturbed at smaller tip-molecule separations, the observation of dI/dV in the limit $\Gamma_2 \ll \Gamma_1$ was not possible.

The above analysis for CuPc^- can be similarly applied to the case of conduction through CuPc^+ (molecule M3, Fig. 4), where the molecule loses one electron to become CuPc^+ , instead of gaining one electron.

The presented data show that the asymmetry of tunneling rates in a double-barrier single-molecule junction can have a profound effect on the I - V characteristics. The effect was demonstrated for vibronic levels associated with the affinity (CuPc^-) and ionization (CuPc^+) states of CuPc. These results can be extended to the understanding of a general class of two-step electron transfer phenomena.

This material is based on work supported by the Chemical Science, Geo- and Bioscience Division, Office of Science, U.S. Department of Energy (Grant No. DE-FG03-01ER15157) and the National Science Foundation (Grant No. 0102887).

*Corresponding author.

Electronic address: wilsonho@uci.edu

- [1] A. Nitzan and M. A. Ratner, *Science* **300**, 1384 (2003).
- [2] J. Park *et al.*, *Nature (London)* **417**, 722 (2002).
- [3] H. Park *et al.*, *Nature (London)* **407**, 57 (2000).
- [4] W. Liang *et al.*, *Nature (London)* **417**, 725 (2002).
- [5] S. Kubatkin *et al.*, *Nature (London)* **425**, 698 (2003).
- [6] J. Reichert *et al.*, *Phys. Rev. Lett.* **88**, 176804 (2002).
- [7] B. Xu and N. J. Tao, *Science* **301**, 1221 (2003).
- [8] X. D. Cui *et al.*, *Science* **294**, 571 (2001).
- [9] P. Jarillo-Herrero *et al.*, *Nature (London)* **429**, 389 (2004).
- [10] D. Katz, O. Millo, S.-H. Kan, and U. Banin, *Appl. Phys. Lett.* **79**, 117 (2001).
- [11] B. Su, V. J. Goldman, and J. E. Cunningham, *Science* **255**, 313 (1992).
- [12] X. H. Qiu, G. V. Nazin, and W. Ho, *Phys. Rev. Lett.* **92**, 206102 (2004).
- [13] A. Stierle *et al.*, *Science* **303**, 1652 (2004).
- [14] S. Datta *et al.*, *Phys. Rev. Lett.* **79**, 2530 (1997).
- [15] In comparison, vibrations in inelastic electron tunneling spectroscopy are observed at the threshold voltages corresponding to the vibrational energies for single molecules adsorbed on a conducting substrate. Tunneling occurs through the vacuum barrier in a one-step process. [B. C. Stipe, M. A. Rezaei, and W. Ho, *Science* **280**, 1732 (1998)].
- [16] B. C. Stipe, M. A. Rezaei, and W. Ho, *Rev. Sci. Instrum.* **70**, 137 (1999).
- [17] B. J. Palys *et al.*, *J. Raman Spectrosc.* **26**, 63 (1995).
- [18] S. Braig and K. Flensberg, *Phys. Rev. B* **68**, 205324 (2003).
- [19] H. Sumi, *J. Phys. Chem. B* **102**, 1833 (1998).
- [20] All the dI/dV curves are scaled and offset for clarity. The peak intensities at $V_b > 0$ and $V_b < 0$ show the same z dependence as the data displayed in Fig. 3(f).
- [21] G. C. Schatz and M. A. Ratner, *Quantum Mechanics in Chemistry* (Prentice Hall, Englewood Cliffs, NJ, 1993).